

**PREPARATION, CHARACTERISATION AND ADSORPTION
PROPERTIES OF CHITOSAN AND CHITOSAN DERIVATIVES BEADS
FOR THE REMOVAL OF COPPER(II) AND LEAD(II) IONS**

by

SHARON D/O FATINATHAN

**This thesis submitted in fulfillment of the requirements for the degree of Doctor of
Philosophy**

July 2010

ACKNOWLEDGEMENTS

It gives me great pleasure to acknowledge the dedicated Associate Professor Dr. Wan Saime Wan Ngah for his invaluable teaching and guidance throughout the research. His professionalism helped me each time I stumbled upon an unexpected twist or turn in my research. I would like to express my gratitude to Universiti Sains Malaysia as my PhD study was funded under the Universiti Sains Malaysia's Fellowship Scheme.

I am deeply grateful to Mr. Ariffin, Mr. Aw Yeong, Mrs. Saripah Mansur, Mr. Muthu, Mr. Kanthasamy, Mr. Johari (School of Biological Sciences) and Ms. Jamilah (School of Biological Sciences) for their technical support in using the instruments required to complete my research.

Many thanks also go to Dr. Oo Chuan Wei, Dr. Megat, Mr. Lim Eng Khoon, Ms. Noorul, Mr. Muhammad Anwar, Mrs. Roslinda, Ms. Sangeetha and Mrs. Puteri Shakira for their friendship and valuable comments and suggestions which helped me during my study.

Finally, to my parents (Mr. Fatinathan and Mrs. Reginnamary) who endured me at times when I felt low and giving me the support I needed to hold on until the end of this research. Unlimited thanks are given especially to my mother, for helping me to find the courage that I thought I never had in myself. Thank you.

TABLE OF CONTENTS

	Page
Acknowledgements	ii
Table of Contents	iii
List of Tables	ix
List of Figures	xii
List of Abbreviations and Symbols	xx
Abstrak	xxiii
Abstract	xxv
 CHAPTER ONE – INTRODUCTION	
1.1 Pollution	1
1.2 Heavy Metals	2
1.2.1 Copper	3
1.2.2 Lead	5
1.3 Treatment Technologies for Heavy Metal Ions Containing Wastewaters	6
1.3.1 Chemical precipitation	7
1.3.2 Ion exchange	8
1.3.3 Electrocoagulation	9
1.3.4 Reverse osmosis	10
1.3.5 Electrodialysis	12
1.3.6 Adsorption	13
1.4 Sources and Properties of Chitin	16
1.5 Chitosan	20
1.5.1 Properties of chitosan	21

1.5.2	Applications of chitosan	23
1.6	Modifications of Chitosan	
1.6.1	Physical modification of chitosan	24
1.6.2	Chemical modification of chitosan	25
1.6.3	Polyelectrolyte complex of chitosan	26
1.6.4	Ionic cross-linking of chitosan	30
1.7	Adsorption and Equilibrium Isotherm Models	32
1.8	Adsorption Kinetic Models	36
1.9	Research Objectives	38

CHAPTER TWO – MATERIALS AND METHODS

2.1	List of Chemicals and Instruments	
2.1.1	Chemicals	40
2.1.2	Instruments	41
2.2	Determination of the Degree of Deacetylation of Chitosan Flakes	42
2.3	Preparation of Chitosan Beads	43
2.4	Preparation of Chitosan-Glutaraldehyde (Chitosan-GLA) Beads	45
2.5	Preparation of Chitosan-Alginate Beads	47
2.6	Preparation of Chitosan-Tripolyphosphate (Chitosan-TPP) Beads	49
2.7	Preparation of Stock Solutions	
2.7.1	Stock solution of 1000 mg/L of copper(II) ions	51
2.7.2	Stock solution of 500 mg/L of lead(II) ions	51
2.7.3	Stock solution of 10000 mg/L of cesium(II) chloride	51
2.7.4	Stock solution of 5 % (w/v) of lanthanum nitrate hexahydrate	52
2.8	Characterization of Chitosan, Chitosan-GLA (1:1 and 1:2), Chitosan-Alginate and Chitosan-TPP Beads	

2.8.1	Fourier transform infrared (FTIR) spectroscopy	52
2.8.2	Light metal cations analysis	52
2.8.3	Surface area and pore size analysis	53
2.8.4	Carbon, hydrogen and nitrogen (CHN) analysis	54
2.8.5	Scanning electron microscopy (SEM) and energy dispersive X-ray (EDX) analyzer	54
2.8.6	X-ray diffraction (XRD) analysis	55
2.8.7	Determination of point of zero charge (pH_{pzc})	55
2.9	Dissolution and Swelling Test for Chitosan, Chitosan-GLA (1:1 and 1:2), Chitosan-Alginate and Chitosan-TPP Beads	56
2.10	Batch Adsorption Experiments	57
2.10.1	Determination of precipitation pH of copper(II) and lead(II) hydroxide	57
2.10.2	Determination of optimum pH	58
2.10.3	Determination of optimum agitation period	58
2.10.4	Determination of optimum agitation rate	59
2.10.5	Determination of optimum particle size	60
2.10.6	Determination of optimum adsorbent dosage	61
2.11	Isotherm Studies	62
2.12	Competitive Adsorption in Binary Metal System	62
2.13	Desorption and Regeneration Study	63
2.14	Determination of Precision for Adsorption Study	64
2.15	Ion Exchange Study	64
 CHAPTER 3 - RESULTS AND DISCUSSION		
3.1	Degree of Deacetylation of Chitosan Flakes	66
3.2	Preparation of Chitosan Beads	72

3.3	Preparation of Chitosan-Glutaraldehyde (GLA) Beads	75
3.4	Preparation of Chitosan-Alginate Beads	80
3.5	Preparation of Chitosan-Tripolyphosphate (Chitosan-TPP) Beads	82
3.6	Characterization of Chitosan, Chitosan-GLA (1:1 and 1:2), Chitosan-Alginate and Chitosan-TPP Beads	
3.6.1	Light metal cations analysis	86
3.6.2	Surface area and pore size analysis	87
3.6.3	Carbon, hydrogen and nitrogen (CHN) elemental analysis	89
3.6.4	Scanning electron microscope (SEM) and energy dispersive X-ray (EDX) analysis	90
3.6.5	X-ray diffraction (XRD) analysis	93
3.6.6	Determination of point of zero charge (pH_{pzc})	95
3.7	Dissolution and Swelling Test for Chitosan, Chitosan-GLA (1:1 and 1:2), Chitosan-Alginate and Chitosan-TPP Beads	97
3.8	Adsorption of Copper(II) and Lead(II) ions onto Chitosan, Chitosan-GLA (1:1 and 1:2), Chitosan-Alginate and Chitosan-TPP Beads	101
3.8.1	Determination of copper(II) and lead(II) hydroxide formation	102
3.8.2	Effect of initial pH on the adsorption of copper(II) and lead(II) ions onto chitosan, chitosan-GLA (1:1 and 1:2), chitosan-alginate and chitosan-TPP beads	106
3.8.3	Effect of agitation period on the adsorption of copper(II) and lead(II) ions onto chitosan, chitosan-GLA (1:1 and 1:2), chitosan-alginate and chitosan-TPP beads	112
3.8.4	Effect of agitation rate on the adsorption of copper(II) and lead(II) ions onto chitosan, chitosan-GLA (1:1 and 1:2), chitosan-alginate and chitosan-TPP beads	114
3.8.5	Effect of particle sizes on the adsorption of copper(II) and lead(II) ions onto chitosan, chitosan-GLA (1:1 and 1:2), chitosan-alginate and chitosan-TPP beads	116

3.8.6	Effect of adsorbent dosage on the adsorption of copper(II) and lead(II) ions onto chitosan, chitosan-GLA (1:1 and 1:2), chitosan-alginate and chitosan-TPP beads	119
3.9	Adsorption Isotherms	
3.9.1	Effect of initial concentration on the adsorption of copper(II) and lead(II) ions onto chitosan, chitosan-GLA (1:1 and 1:2), chitosan-alginate and chitosan-TPP beads	122
3.9.2	Langmuir isotherm model	127
3.9.3	Freundlich isotherm model	136
3.9.4	Dubinin-Radushkevich (D-R) isotherm model	140
3.9.5	Sips isotherm model	143
3.9.6	Redlich-Peterson (R-P) isotherm model	146
3.10	Thermodynamics of the Adsorption Process	150
3.11	Kinetics Study	164
3.11.1	Pseudo first-order kinetic model	164
3.11.2	Pseudo second-order kinetic model	169
3.11.3	Intraparticle diffusion model	173
3.12	Binary Studies	178
3.13	Mutual Displacement of Copper(II) and Lead(II) Ions	185
3.14	Adsorption-Desorption (Regeneration Study)	187
3.15	Determination of Precision for Adsorption Study	196
3.16	Adsorption Mechanism	197
3.16.1	Infrared spectroscopy analysis	198
3.16.2	Scanning electron microscope (SEM) and energy dispersive X-ray (EDX) analysis	204
3.16.3	Effect of pH on the adsorption of copper(II) and lead(II) ions onto chitosan, chitosan-GLA (1:1 and 1:2), chitosan-alginate and chitosan-TPP beads	211

3.16.4	Effect of ion-exchange process on the adsorption of copper (II) and lead(II) ions onto chitosan, chitosan-GLA (1:1 and 1:2), chitosan-alginate and chitosan-TPP beads	214
3.16.5	Proposed structures for the adsorption of copper(II) and lead(II) ions	220
CHAPTER FOUR – CONCLUSION		229
CHAPTER FIVE - RECOMMENDATIONS FOR FUTURE RESEARCH		234
REFERENCES		235
LIST OF PUBLICATIONS		

LIST OF TABLES

		Page
Table 1.1	Proportions of organic components in arthropod cuticles (Muzzarelli, 1973)	18
Table 1.2	Key properties of chitosan (Sandford and Hutchings, 1987; Crini and Badot, 2008)	22
Table 1.3	Equilibrium isotherm models used in this study (Aksu, 2005; Gerente et al., 2007; Crini and Badot, 2008; Febrianto et al., 2009)	36
Table 1.4	Kinetic models used in this study (Ho and McKay, 1998; Li et al., 2009)	37
Table 3.1	Summary of infrared absorption band for chitosan flakes and chitosan beads	74
Table 3.2	Summary of infrared absorption band for chitosan-TPP beads	85
Table 3.3	Composition of light metal cations found in chitosan, chitosan-GLA (1:1 and 1:2), chitosan-alginate and chitosan-TPP beads	87
Table 3.4	Physical characteristics of chitosan, chitosan-GLA (1:1 and 1:2), chitosan-alginate and chitosan-TPP beads	88
Table 3.5	Percentage of carbon, hydrogen and nitrogen, and the C/N ratio for chitosan, chitosan-GLA (1:1 and 1:2), chitosan-alginate and chitosan-TPP beads	90
Table 3.6	Dissolution effect of chitosan, chitosan-GLA (1:1 and 1:2), chitosan-alginate and chitosan-TPP beads in different medium	98
Table 3.7	Swelling behaviour of chitosan, chitosan-GLA (1:1 and 1:2), chitosan-alginate and chitosan-TPP beads in different medium	98
Table 3.8	Optimum agitation period for the adsorption of copper(II) and lead(II) ions onto chitosan, chitosan-GLA (1:1 and 1:2), chitosan-alginate and chitosan-TPP beads	114
Table 3.9	Optimum adsorbent dosage used for the adsorption of copper(II) and lead(II) ions onto chitosan, chitosan-GLA (1:1 and 1:2), chitosan-alginate and chitosan-TPP beads	122

Table 3.10	Langmuir isotherm constants, correlation coefficients (R^2) and the residual root mean square errors ($RMSE$) for the adsorption of copper(II) and lead(II) ions onto chitosan, chitosan-GLA (1:1 and 1:2), chitosan-alginate and chitosan-TPP beads	130
Table 3.11	Comparison of adsorption capacities of copper(II) and lead(II) ions with other reported adsorbents based on the adsorption capacity at complete monolayer, V_m	133
Table 3.12	Freundlich isotherm constants, correlation coefficients (R^2) and the residual root mean square errors ($RMSE$) for the adsorption of copper(II) and lead(II) ions onto chitosan, chitosan-GLA (1:1 and 1:2), chitosan-alginate and chitosan-TPP beads	138
Table 3.13	D-R isotherm constants, correlation coefficients (R^2) and the residual root mean square errors ($RMSE$) for the adsorption of copper(II) and lead(II) ions onto chitosan, chitosan-GLA (1:1 and 1:2), chitosan-alginate and chitosan-TPP beads	143
Table 3.14	Sips isotherm constants, correlation coefficients (R^2) and the residual root mean square errors ($RMSE$) for the adsorption of copper(II) and lead(II) ions onto chitosan, chitosan-GLA (1:1 and 1:2), chitosan-alginate and chitosan-TPP beads	146
Table 3.15	R-P isotherm constants, correlation coefficients (R^2) and the residual root mean square errors ($RMSE$) for the adsorption of copper(II) and lead(II) ions onto chitosan, chitosan-GLA (1:1 and 1:2), chitosan-alginate and chitosan-TPP beads	149
Table 3.16	Langmuir and Freundlich isotherm constants, correlation coefficients (R^2) and the residual root mean square errors ($RMSE$) for the adsorption of copper(II) ions onto chitosan, chitosan-GLA (1:1 and 1:2), chitosan-alginate and chitosan-TPP beads at different temperature	153
Table 3.17	Langmuir and Freundlich isotherm constants, correlation coefficients (R^2) and the residual root mean square errors ($RMSE$) for the adsorption of lead(II) ions onto chitosan, chitosan-GLA (1:1 and 1:2), chitosan-alginate and chitosan-TPP beads at different temperature	155
Table 3.18	Thermodynamics parameters for the adsorption of copper(II) and lead(II) ions onto chitosan, chitosan-GLA (1:1 and 1:2), chitosan-alginate and chitosan-TPP beads	161

Table 3.19	Pseudo first-order kinetic model constants and correlation coefficients (R^2) for the adsorption of copper(II) and lead(II) ions onto chitosan, chitosan-GLA (1:1 and 1:2), chitosan-alginate and chitosan-TPP beads	168
Table 3.20	Pseudo second-order kinetic model constants and correlation coefficients (R^2) for the adsorption of copper(II) and lead(II) ions onto chitosan, chitosan-GLA (1:1 and 1:2), chitosan-alginate and chitosan-TPP beads	173
Table 3.21	Intraparticle diffusion model constants and correlation coefficients (R^2) for the adsorption of copper(II) and lead(II) ions onto chitosan, chitosan-GLA (1:1 and 1:2), chitosan-alginate and chitosan-TPP beads	177
Table 3.22	Langmuir isotherm constants and correlation coefficients (R^2) for the adsorption of copper(II) and lead(II) ions onto chitosan, chitosan-GLA (1:1 and 1:2), chitosan-alginate and chitosan-TPP beads in the binary metal system	181
Table 3.23	Properties of copper(II) and lead(II) ions (Liu et al., 2008)	184
Table 3.24	Mutual displacement of earlier adsorbed copper(II) ions by lead(II) ions	185
Table 3.25	Mutual displacement of earlier adsorbed lead(II) ions by copper(II) ions	186
Table 3.26	Percentage of desorption of copper(II) ions from chitosan, chitosan-GLA (1:1 and 1:2), chitosan-alginate and chitosan-TPP beads using different desorption agent	189
Table 3.27	Percentage of desorption of lead(II) ions from chitosan, chitosan-GLA (1:1 and 1:2), chitosan-alginate and chitosan-TPP beads using different desorption agent	190
Table 3.28	pH values obtained for chitosan, chitosan-GLA (1:1 and 1:2), chitosan-alginate and chitosan-TPP beads at different time intervals during the adsorption of copper(II) and lead(II) ions	213
Table 3.29	Concentration of metal cations released from chitosan, chitosan-GLA (1:1 and 1:2), chitosan-alginate and chitosan-TPP beads in distilled water	215
Table 3.30	The $R_{b/r}$ values obtained for chitosan, chitosan-GLA (1:1 and 1:2), chitosan-alginate and chitosan-TPP beads during the adsorption of copper(II) and lead(II) ions	219

LIST OF FIGURES

		Page
Figure 1.1	Structures of (a) cellulose, (b) chitin and (c) chitosan	17
Figure 1.2	Classification of adsorption isotherms of solids from solution (Giles et al., 1974)	34
Figure 2.1	Schematic diagram on the preparation of chitosan beads	44
Figure 2.2	Schematic diagram on the preparation of chitosan-GLA beads	46
Figure 2.3	Schematic diagram on the preparation of chitosan-alginate beads	48
Figure 2.4	Schematic diagram on the preparation of chitosan-TPP beads	50
Figure 3.1	Mechanism for the preparation of chitosan from chitin (deacetylation process)	67
Figure 3.2	FTIR spectra of chitosan flakes and the calculation procedure to determine the degree of deacetylation for chitosan flakes	69
Figure 3.3	pH-potentiometric titration curve for chitosan flakes	70
Figure 3.4	First order derivative plot based on pH-potentiometric titration curve for chitosan flakes	71
Figure 3.5	FTIR spectrum of chitosan flakes and chitosan beads	74
Figure 3.6	Mechanism for the formation of Schiff base (Roberts and Taylor, 1989; Wade Jr, 2006)	75
Figure 3.7	FTIR spectrum of chitosan beads and chitosan-GLA 1:1 beads	76
Figure 3.8	FTIR spectrum of chitosan-GLA 1:1 and chitosan-GLA 1:2 beads	78
Figure 3.9	The formation of ethylenic bond (C=C) (Neckers and Doyle, 1977)	78
Figure 3.10	The structure of cross-linked chitosan beads using glutaraldehyde (GLA)	79

Figure 3.11	The structure of polyelectrolyte complex, chitosan-alginate beads	81
Figure 3.12	FTIR spectrum of chitosan-beads and chitosan-alginate beads	82
Figure 3.13	The formation of chitosan-tripolyphosphate (Chitosan-TPP) beads	84
Figure 3.14	Comparison of FTIR spectrum of chitosan beads and chitosan-TPP beads	85
Figure 3.15	SEM-EDX micrographs obtained for (a) chitosan, (b) chitosan-GLA 1:1, (c) chitosan-GLA 1:2, (d) chitosan-alginate and (e) chitosan-TPP beads; at 5000x	91
Figure 3.16	XRD micrographs obtained for (a) chitosan, (b) chitosan-GLA 1:1, (c) chitosan-GLA 1:2, (d) chitosan-alginate and (e) chitosan-TPP beads	94
Figure 3.17	pH_{pzc} obtained for chitosan flakes, chitosan, chitosan-GLA 1:1, chitosan-GLA 1:2, chitosan-alginate and chitosan-TPP beads	96
Figure 3.18	(a) Effect of pH on the formation of copper(II) ions and (b) zone of predominant for copper species (Nurchi and Villaescusa, 2008)	103
Figure 3.19	(a) Effect of pH on the formation of lead(II) ions and (b) zone of predominant for lead species in high concentration of metal ions and (c) lead species in low concentration of metal ions (Nurchi and Villaescusa, 2008)	105
Figure 3.20	Effect of pH on the adsorption of copper(II) ions onto chitosan, chitosan-GLA (1:1 and 1:2), chitosan-alginate and chitosan-TPP beads	108
Figure 3.21	Effect of pH on the adsorption of lead(II) ions onto chitosan, chitosan-GLA (1:1 and 1:2), chitosan-alginate and chitosan-TPP beads	108
Figure 3.22	The effect of pH on the adsorption of metal ions onto chitosan-TPP beads	111
Figure 3.23	Effect of agitation period on the adsorption of copper(II) ions onto chitosan, chitosan-GLA (1:1 and 1:2), chitosan-alginate and chitosan-TPP beads	113

Figure 3.24	Effect of agitation period on the adsorption of lead(II) ions onto chitosan, chitosan-GLA (1:1 and 1:2), chitosan-alginate and chitosan-TPP beads	113
Figure 3.25	Effect of agitation rate on the adsorption of copper(II) ions onto chitosan, chitosan-GLA (1:1 and 1:2), chitosan-alginate and chitosan-TPP beads	115
Figure 3.26	Effect of agitation rate on the adsorption of lead(II) ions onto chitosan, chitosan-GLA (1:1 and 1:2), chitosan-alginate and chitosan-TPP beads	116
Figure 3.27	Effect of particle size on the adsorption capacity of copper(II) ions onto chitosan, chitosan-GLA (1:1 and 1:2), chitosan-alginate and chitosan-TPP beads	117
Figure 3.28	Effect of particle size on the adsorption capacity of lead(II) ions onto chitosan, chitosan-GLA (1:1 and 1:2), chitosan-alginate and chitosan-TPP beads	118
Figure 3.29	Effect of adsorbent dosage on the percentage of removal of copper(II) ions by chitosan, chitosan-GLA (1:1 and 1:2), chitosan-alginate and chitosan-TPP beads	120
Figure 3.30	Effect of adsorbent dosage on the percentage of removal of lead(II) ions by chitosan, chitosan-GLA (1:1 and 1:2), chitosan-alginate and chitosan-TPP beads	120
Figure 3.31	Effect of adsorbent dosage on the adsorption capacity of copper(II) ions by chitosan, chitosan-GLA (1:1 and 1:2), chitosan-alginate and chitosan-TPP beads	121
Figure 3.32	Effect of adsorbent dosage on the adsorption capacity of lead(II) ions by chitosan, chitosan-GLA (1:1 and 1:2), chitosan-alginate and chitosan-TPP beads	121
Figure 3.33	Equilibrium adsorption isotherm for the adsorption of copper(II) and lead(II) ions onto chitosan beads	124
Figure 3.34	Equilibrium adsorption isotherm for the adsorption of copper(II) and lead(II) ions onto chitosan-GLA 1:1 beads	124
Figure 3.35	Equilibrium adsorption isotherm for the adsorption of copper(II) and lead(II) ions onto chitosan-GLA 1:2 beads	125
Figure 3.36	Equilibrium adsorption isotherm for the adsorption of copper(II) and lead(II) ions onto chitosan-alginate beads	125
Figure 3.37	Equilibrium adsorption isotherm for the adsorption of copper(II) and lead(II) ions onto chitosan-TPP beads	126

Figure 3.38	Non-linear Langmuir isotherm for the adsorption of copper (II) ions onto chitosan, chitosan-GLA (1:1 and 1:2), chitosan-alginate and chitosan-TPP beads	129
Figure 3.39	Non-linear Langmuir isotherm for the adsorption of lead(II) ions onto chitosan, chitosan-GLA (1:1 and 1:2), chitosan-alginate and chitosan-TPP beads	129
Figure 3.40	Plot of R_L against initial metal concentration of copper(II) ions for chitosan, chitosan-GLA (1:1 and 1:2), chitosan-alginate and chitosan-TPP beads	135
Figure 3.41	Plot of R_L against initial metal concentration of lead(II) ions for chitosan, chitosan-GLA (1:1 and 1:2), chitosan-alginate and chitosan-TPP beads	135
Figure 3.42	Non-linear Freundlich isotherm for the adsorption of copper(II) ions onto chitosan, chitosan-GLA (1:1 and 1:2), chitosan-alginate and chitosan-TPP beads	137
Figure 3.43	Non-linear Freundlich isotherm for the adsorption of lead(II) ions onto chitosan, chitosan-GLA (1:1 and 1:2), chitosan-alginate and chitosan-TPP beads	137
Figure 3.44	Non-linear D-R isotherm for the adsorption of copper(II) ions onto chitosan, chitosan-GLA 1:1, chitosan-alginate and chitosan-TPP beads; Inset: Non-linear D-R isotherm for the adsorption of copper(II) ions onto chitosan-GLA 1:2 beads	141
Figure 3.45	Non-linear D-R isotherm for the adsorption of lead(II) ions onto chitosan, chitosan-GLA (1:1 and 1:2), chitosan-alginate and chitosan-TPP beads	142
Figure 3.46	Non-linear Sips isotherm for the adsorption of copper(II) ions onto chitosan, chitosan-GLA (1:1 and 1:2), chitosan-alginate and chitosan-TPP beads	144
Figure 3.47	Non-linear Sips isotherm for the adsorption of lead(II) ions onto chitosan, chitosan-GLA (1:1 and 1:2), chitosan-alginate and chitosan-TPP beads	145
Figure 3.48	Non-linear R-P isotherm for the adsorption of copper(II) ions onto chitosan, chitosan-GLA (1:1 and 1:2), chitosan-alginate and chitosan-TPP beads	148
Figure 3.49	Non-linear R-P isotherm for the adsorption of lead(II) ions onto chitosan, chitosan-GLA (1:1 and 1:2), chitosan-alginate and chitosan-TPP beads	148

Figure 3.50	Non-linear Langmuir and Freundlich isotherms for the adsorption of copper(II) ions onto chitosan, chitosan-GLA (1:1 and 1:2), chitosan-alginate and chitosan-TPP beads at different temperature	151
Figure 3.51	Non-linear Langmuir and Freundlich isotherms for the adsorption of lead(II) ions onto chitosan, chitosan-GLA (1:1 and 1:2), chitosan-alginate and chitosan-TPP beads at different temperature	152
Figure 3.52	van't Hoff's plot for the adsorption of copper(II) and lead (II) ions onto chitosan beads	158
Figure 3.53	van't Hoff's plot for the adsorption of copper(II) and lead (II) ions onto chitosan-GLA 1:1 beads	159
Figure 3.54	van't Hoff's plot for the adsorption of copper(II) and lead (II) ions onto chitosan-GLA 1:2 beads	159
Figure 3.55	van't Hoff's plot for the adsorption of copper(II) and lead (II) ions onto chitosan-alginate beads	160
Figure 3.56	van't Hoff's plot for the adsorption of copper(II) and lead (II) ions onto chitosan-TPP beads	160
Figure 3.57	Pseudo first-order kinetic model plot for the adsorption of copper(II) and lead(II) ions onto chitosan beads	165
Figure 3.58	Pseudo first-order kinetic model plot for the adsorption of copper(II) and lead(II) ions onto chitosan-GLA 1:1 beads	166
Figure 3.59	Pseudo first-order kinetic model plot for the adsorption of copper(II) and lead(II) ions onto chitosan-GLA 1:2 beads	166
Figure 3.60	Pseudo first-order kinetic model plot for the adsorption of copper(II) and lead(II) ions onto chitosan-alginate beads	167
Figure 3.61	Pseudo first-order kinetic model plot for the adsorption of copper(II) and lead(II) ions onto chitosan-TPP beads	167
Figure 3.62	Pseudo second-order kinetic model plot for the adsorption of copper(II) and lead(II) ions onto chitosan beads	170
Figure 3.63	Pseudo second-order kinetic model plot for the adsorption of copper(II) and lead(II) ions onto chitosan-GLA 1:1 beads	170
Figure 3.64	Pseudo second-order kinetic model plot for the adsorption of copper(II) and lead(II) ions onto chitosan-GLA 1:2 beads	171

Figure 3.65	Pseudo second-order kinetic model plot for the adsorption of copper(II) and lead(II) ions onto chitosan-alginate beads	171
Figure 3.66	Pseudo second-order kinetic model plot for the adsorption of copper(II) and lead(II) ions onto chitosan-TPP beads	172
Figure 3.67	Intraparticle diffusion model plot for the adsorption of copper(II) and lead(II) ions onto chitosan beads	174
Figure 3.68	Intraparticle diffusion model plot for the adsorption of copper(II) and lead(II) ions onto chitosan-GLA 1:1 beads	175
Figure 3.69	Intraparticle diffusion model plot for the adsorption of copper(II) and lead(II) ions onto chitosan-GLA 1:2 beads	175
Figure 3.70	Intraparticle diffusion model plot for the adsorption of copper(II) and lead(II) ions onto chitosan-alginate beads	176
Figure 3.71	Intraparticle diffusion model plot for the adsorption of copper(II) and lead(II) ions onto chitosan-TPP beads	176
Figure 3.72	Non-linear Langmuir and Freundlich isotherms for the adsorption of copper(II) and lead(II) ions in binary metal system onto chitosan beads	179
Figure 3.73	Non-linear Langmuir and Freundlich isotherms for the adsorption of copper(II) and lead(II) ions in binary metal system onto chitosan-GLA 1:1 beads	179
Figure 3.74	Non-linear Langmuir and Freundlich isotherms for the adsorption of copper(II) and lead(II) ions in binary metal system onto chitosan-GLA 1:2 beads	180
Figure 3.75	Non-linear Langmuir and Freundlich isotherms for the adsorption of copper(II) and lead(II) ions in binary metal system onto chitosan-alginate beads	180
Figure 3.76	Non-linear Langmuir and Freundlich isotherms for the adsorption of copper(II) and lead(II) ions in binary metal system onto chitosan-TPP beads	181
Figure 3.77	Adsorption capacity for the adsorption of copper(II) ions in single and binary metal system onto chitosan, chitosan-GLA (1:1 and 1:2), chitosan-alginate and chitosan-TPP beads	182
Figure 3.78	Adsorption capacity for the adsorption of lead(II) ions in single and binary metal system onto chitosan, chitosan-GLA (1:1 and 1:2), chitosan-alginate and chitosan-TPP beads	182

Figure 3.79	The formation of ethylenediaminetetraacetic acid (EDTA)	188
Figure 3.80	Percentage of removal and desorption of copper(II) ions onto chitosan, chitosan-GLA (1:1 and 1:2), chitosan-alginate and chitosan-TPP beads	192
Figure 3.81	Percentage of removal and desorption of lead(II) ions onto chitosan, chitosan-GLA (1:1 and 1:2), chitosan-alginate and chitosan-TPP beads	194
Figure 3.82	FTIR spectrum of chitosan beads before and after the adsorption of copper(II) and lead(II) ions	199
Figure 3.83	FTIR spectrum of chitosan-GLA 1:1 beads before and after the adsorption of copper(II) and lead(II) ions	201
Figure 3.84	FTIR spectrum of chitosan-GLA 1:2 beads before and after the adsorption of copper(II) and lead(II) ions	201
Figure 3.85	FTIR spectrum of chitosan-alginate beads before and after the adsorption of copper(II) and lead(II) ions	202
Figure 3.86	FTIR spectrum of chitosan-TPP beads before and after the adsorption of copper(II) and lead(II) ions	203
Figure 3.87	SEM-EDX micrographs obtained after the adsorption of copper(II) ions onto (a) chitosan (b) chitosan-GLA 1:1 (c) chitosan-GLA 1:2 (d) chitosan-alginate (e) chitosan-TPP beads; at 1000x	205
Figure 3.88	SEM-EDX micrographs obtained after the adsorption of lead(II) ions onto (a) chitosan (b) chitosan-GLA 1:1 (c) chitosan-GLA 1:2 (d) chitosan-alginate and (e) chitosan-TPP beads; at 1000x	207
Figure 3.89	SEM-EDX micrographs obtained after the adsorption of copper(II) and lead(II) ions in the binary metal system onto (a) chitosan (b) chitosan-GLA 1:1 (c) chitosan-GLA 1:2 (d) chitosan-alginate (e) chitosan-TPP beads; at 1000x	209
Figure 3.90	Spot analysis on the star shaped particles found on the surface chitosan-alginate beads	210
Figure 3.91	Adsorption of copper(II) ions and displacement of Na ⁺ , K ⁺ , Ca ²⁺ and Mg ²⁺ by chitosan, chitosan-GLA (1:1 and 1:2), chitosan-alginate and chitosan-TPP beads	217
Figure 3.92	Adsorption of lead(II) ions and displacement of Na ⁺ , K ⁺ , Ca ²⁺ and Mg ²⁺ by chitosan, chitosan-GLA (1:1 and 1:2), chitosan-alginate and chitosan-TPP beads	218

Figure 3.93	Proposed mechanism for the adsorption of metal ions (M^{2+}) onto chitosan beads in neutral or slightly acidic metal ions solution	222
Figure 3.94	Proposed mechanism for the adsorption of metal ions (M^{2+}) onto chitosan beads in acidic metal ions solution	223
Figure 3.95	Proposed mechanism for the adsorption of metal ions (M^{2+}) onto chitosan-GLA (1:1 and 1:2) beads	224
Figure 3.96	Proposed mechanism for the adsorption of metal ions (M^{2+}) onto chitosan-alginate beads	226
Figure 3.97	Proposed mechanism for the adsorption of metal ions (M^{2+}) onto chitosan-TPP beads	228

LIST OF ABBREVIATIONS AND SYMBOLS

$1/n$	The heterogeneity factor based on Sips isotherm model
ΔG°	Gibbs free energy change
ΔH°	Enthalpy change
ΔS°	Entropy change
ε	A Polanyi potential whereby it is $[RT \ln (1 + (1 / C_e))]$
A and B	The Redlich-Peterson isotherm constant (L/g) and $(L/mg)^{1/n}$, respectively
A	Absorbance
AAS	Atomic absorption spectrophotometer
BET	Brunauer-Emmett-Teller
BJH	Barett, Joyner and Halenda
b_L	The Langmuir constant related to the affinity of binding sites (L/mg)
b_S	The median association constant (mL/mg)
C_e	The final/equilibrium concentration of copper(II) or lead(II) ions (mg/L)
CHN	Carbon, hydrogen and nitrogen
C_o	The initial concentration of copper(II) or lead(II) ions (mg/L)
D-R	Dubinin-Radushkevich
E	The mean free energy of adsorption per molecule of the adsorbate (kJ/mol)
ECH	Epichlorohydrin
EDTA	Ethylenediaminetetraacetic acid
EDX	Energy dispersive X-ray spectrometer
EGDE	Ethylene glycol diglycidyl ether
FTIR	Fourier transform infrared spectroscopy
g	The exponent (heterogeneity factor) based on R-P isotherm model

GLA	Glutaraldehyde
h_o	The initial height of the beads (cm)
h_t	The height of swollen beads (cm) at time t
IUPAC	International Union of Pure and Applied Chemistry
k	A constant related to the adsorption energy (mol^2/kJ^2)
k_1	The rate constant of pseudo first-order kinetic model (min^{-1})
k_2	The rate constant of pseudo-second order kinetic model ($\text{g}/\text{mg min}$)
K_F	A constant characterizing the adsorption capacity ($(\text{mg}/\text{g}) (\text{L}/\text{mg})^{1/n}$) of the adsorbent
$k_{int,i}$	The intraparticle diffusion rate constant ($\text{mg g}^{-1} \text{min}^{-1/2}$) ($i = 1-2$)
K_{sp}	Solubility constant
M^{2+}	The concentration of metal ions (copper(II) or lead(II)) adsorbed in mmol/L
M_{NaOH}	The molarity of the NaOH solution (M)
n	An empirical parameter related to the intensity of adsorption
Na_2EDTA	Disodium ethylenediaminetetraacetic acid salt
NMR	Nuclear Magnetic Resonance
pH_{pzc}	Point of zero charge
Q	The amount of solute adsorbed per unit weight of adsorbent (mol/g)
Q_{DR}	The adsorption capacity (mol/g) based on D-R isotherm model
q_e	Adsorption capacity (amount of metal ions adsorbed per mass unit of adsorbent at equilibrium) (mg/g)
q_e, q_t	The amounts of copper(II) and lead(II) ions adsorbed onto the adsorbents (mg/g) at equilibrium and at time t
q_s	The total number of binding sites (mg/g)
R	The gas constant ($8.314 \text{ J}/\text{K mol}$)
R^2	Correlation coefficients

$R_{b/r}$	Ratio used for ion exchange study
R_L	The dimensionless constant separation factor
$RMSE$	Residual root mean square errors
R-P	Redlich-Peterson
rpm	Rotations per minute
RSD	Relative standard deviation
S	Percentage of swelling (%)
SD	Standard deviation
SEM	Scanning electron microscope
SPVDF	Sulfonated polyvinylidene fluoride membrane
STPP	Sodium tripolyphosphate
T	The temperature in Kelvin (K)
t	Time (min)
TPP	Tripolyphosphate
UV	Ultraviolet
V	The volume of copper(II) and lead(II) ions solution (mL)
V_1, V_2	The volume (L) of NaOH used to neutralize the excess of HCl
V_m	The maximum adsorption capacity at complete monolayer (mg/g)
W	The weight of the adsorbent (g) used
W_2	The mass of chitosan flakes (g)
WHO	World Health Organization
XPS	X-ray photoelectron spectroscopy
XRD	X-ray diffraction

**PENYEDIAAN, PENCIRIAN DAN SIFAT-SIFAT PENJERAPAN MANIK
KITOSAN DAN TERBITAN KITOSAN UNTUK PENYINGKIRAN ION
KUPRUM(II) DAN PLUMBUM(II)**

ABSTRAK

Dalam kajian ini, sistem penjerapan kelompok telah digunakan untuk mengkaji penjerapan ion kuprum(II) dan plumbum(II) ke atas manik kitosan, manik kitosan-glutaraldehyd (GLA) (1:1 dan 1:2), manik kitosan-alginat dan manik kitosan-tripolifosfat (TPP) telah dikaji. Sifat-sifat fizikokimia bagi kelima-lima penjerap tersebut telah dianalisis dengan menggunakan kaedah spektroskopi inframerah, analisis kandungan ion-ion logam ringan, analisis luas permukaan dan saiz liang, analisis kandungan CHN dan analisis pembelauan sinar-X. Beberapa parameter yang memberi kesan terhadap nilai muatan penjerapan seperti pH, tempoh pengacauan, kelajuan pengacauan, saiz zarah, dos bahan penjerap, kepekatan awal ion logam dan suhu telah dikaji. Data isoterma penjerapan bagi ion kuprum(II) dan plumbum(II) ke atas kelima-lima penjerap tersebut telah ditentukan dan dipadankan dengan model-model isoterma seperti Langmuir, Freundlich, Dubinin-Radushkevich (D-R), Sips dan Redlich-Peterson (R-P). Muatan penjerapan maksimum untuk manik kitosan, manik kitosan-GLA 1:1, manik kitosan-GLA 1:2, manik kitosan-alginat dan manik kitosan-TPP berdasarkan isoterma Langmuir ialah masing-masing 64.62, 29.95, 22.16, 67.66 dan 24.19 mg/g untuk ion kuprum(II) dan masing-masing 34.98, 15.08, 13.71, 60.27 dan 43.25 mg/g untuk ion plumbum(II). Berdasarkan kajian termodinamik, perubahan entalpi (ΔH°) yang diperolehi untuk kelima-lima penjerap bagi penjerapan ion kuprum(II) dan plumbum(II) adalah bersifat endotermik. Apabila suhu sistem ditingkatkan, nilai tenaga bebas Gibbs (ΔG°) yang diperolehi

adalah negatif. Ini menunjukkan proses penjerapan berlaku secara spontan pada suhu tinggi. Model kinetik tertib pseudo-pertama dan pseudo-kedua telah digunakan untuk menganalisis data kinetik. Kelima-lima penjerap menunjukkan nilai korelasi yang baik untuk model kinetik tertib pseudo-kedua yang mengesahkan bahawa penjerapan kimia merupakan langkah pengawalan kadar. Berdasarkan kajian pembauran antara partikel, didapati proses penjerapan ion kuprum(II) dan plumbum(II) adalah kompleks dimana pembauran antara partikel juga menyumbang kepada langkah penentuan kadar. Di dalam sistem binari, kehadiran ion kuprum(II) telah merencatkan proses penjerapan ion plumbum(II). Ini menunjukkan ion kuprum(II) adalah pesaing yang kuat untuk ion plumbum(II). Berdasarkan kajian proses penukaran ion, didapati bahawa proses ini merupakan salah satu daripada mekanisme yang penting dalam proses penjerapan ion kuprum(II) dan plumbum(II) pada kepekatan awal ion logam yang rendah. Apabila kepekatan awal ion logam meningkat, proses pembentukan kompleks serta mekanisme penjerapan yang lain akan memainkan peranan yang lebih penting semasa proses penjerapan ion kuprum(II) dan plumbum(II). Kelima-lima penjerap menunjukkan proses kebolehlulangan yang baik terhadap ion kuprum(II) dan plumbum(II) kerana nilai RSD adalah kurang daripada 5 %. Ion-ion logam berat yang terjerap ke atas kelima-lima penjerap boleh dikembalikan semula dengan menggunakan larutan Na_2EDTA dan digunakan semula sebanyak tiga kali berturut-turut.

**PREPARATION, CHARACTERISATION AND ADSORPTION
PROPERTIES OF CHITOSAN AND CHITOSAN DERIVATIVES BEADS
FOR THE REMOVAL OF COPPER(II) AND LEAD(II) IONS**

ABSTRACT

In this study, a batch adsorption system was applied to study the adsorption of copper(II) and lead(II) ions onto chitosan, chitosan-glutaraldehyde (GLA) (1:1 and 1:2), chitosan-alginate and chitosan-tripolyphosphate (TPP) beads. The physicochemical properties of all five adsorbents were analysed based on infrared spectroscopy, light metal cations analysis, surface area and pore size analysis, CHN analysis and X-ray diffraction analysis. Different parameters affecting the adsorption capacity such as initial pH, agitation period, agitation rate, particle sizes, adsorbent dosage, initial concentration of metal ions and temperature were studied. Adsorption isotherm data for copper(II) and lead(II) ions onto all five adsorbents were determined and correlated with Langmuir, Freundlich, Dubinin-Radushkevich (D-R), Sips and Redlich-Peterson (R-P) isotherm models. The maximum adsorption capacity for chitosan, chitosan-GLA (1:1 and 1:2), chitosan-alginate and chitosan-TPP beads based on Langmuir isotherm were 64.62, 29.95, 22.16, 67.66 and 24.19 mg/g, respectively for copper(II) ions and 34.98, 15.08, 13.71, 60.27 and 43.25 mg/g, respectively for lead(II) ions, in single metal system. Based on thermodynamic studies, the enthalpy change (ΔH°) for all five adsorbents during the adsorption of copper(II) and lead(II) ions were endothermic in nature. As the temperature increased, the Gibbs free energy change (ΔG°) obtained were negative indicating a spontaneous adsorption process at high temperature. Pseudo first- and second-order kinetic models were applied to analyze the kinetic data. All five adsorbents showed

good correlation coefficients for pseudo second-order kinetic model whereby chemical adsorption being the rate controlling step. Based on the intraparticle diffusion, the adsorption process was complex whereby the intraparticle diffusion also contributed to the rate determining step. In the binary metal system, the presence of copper(II) ions caused a reduction in the adsorption of lead(II) ions showing that copper(II) ions were strong competitors for lead(II) ions. Based on the ion-exchange study, it was found that ion-exchange played an important role in the adsorption of copper(II) and lead(II) ions but only at lower initial concentration of the metal ions. As the initial concentration of the metal ions was increased, complexation and other adsorption mechanism played a more crucial role in the adsorption process. All adsorbents showed good reproducibility as the relative standard deviations (RSD) were less than 5 %. All five adsorbents can be effectively regenerated using Na₂EDTA and successfully applied for three successive adsorption-desorption cycles.

CHAPTER ONE

INTRODUCTION

1.1 Pollution

A tremendous growth in the manufacture and use of synthetic chemicals began with the industrial revolution in the middle of 18th century and by the 19th century; pollution became a more noticeable phenomenon. The demands of an increasing population coupled with the desire of most people for a higher standard of living resulted in a worldwide pollution on a massive scale.

Pollution, a word derived from the Latin word “pollutionem”, can be defined as the introduction of substances or energy by human, directly or indirectly into the environment causing hazards to human health, harm to living resources and ecological systems, damage to structure or amenity, or interference with legitimate uses of the environment (Lim and Polprasert, 1996). Virtually all human activities involve the creation of substances and energy. These processes can lead to accidents and the generation of wastes, which can be released accidentally or deliberately into the environment. The possibility of such releases to be categorized as pollution, depend on the critical load present in the ecosystem, or on the acceptable standards for such pollution (Rana, 2006). Environmental pollution can be divided into water, air and soil pollution.

Water, with a deceptively simple chemical formula of H₂O, is an essential part of all living systems and is the medium from which life evolved. However, the

introduction of motorized vehicles and the explosion of human population have caused contamination of water supplies. United States Department of Health Education and Welfare defines water pollution as “the adding of any substance to water, or the changing of water’s physical and chemical characteristics in anyway that interferes with its legitimate purposes” (Rana, 2006). Currently, waterborne toxic chemicals pose the greatest threat to the safety of water supplies in developing nations such as Malaysia. There are many possible sources of chemical contamination. These include wastes from chemical producing industries, metal plating operations and pesticide run off from agricultural lands. The effects of water pollution are not only devastating to humans but also to animals, fish and birds. Polluted water is unsuitable for drinking, recreation, agriculture and industrial use. It also diminishes the aesthetic quality of lakes and rivers. Water pollutants can be divided among some general categories such as inorganic pollutants, trace organic pollutants, trace metals, heavy metals and pesticides (Manahan, 2000).

1.2 Heavy Metals

Environmental contamination and human exposure to heavy metals have dramatically increased in the past 50 years because of their increasing usage in industrial processes and products. Heavy metals are the most harmful of the elemental pollutants and are of particular concern because of their toxicities to humans. There are more than 20 heavy metals and the most harmful metals to human health are mercury, cadmium, lead, arsenic, chromium, copper and zinc (Çavuş and Gürdağ, 2008). The human body cannot metabolize heavy metals and it display bio-accumulative properties causing various diseases and disorders. Metal ions in the

environment can accumulate and are biomagnified along the food chain. Therefore, their toxic effects are more pronounced in animals at higher trophic levels (Ahluwalia and Goyal, 2007).

The most devastating incident involving heavy metals was the organic mercury poisoning which broke out in Minamata Bay area of Japan during the period of 1953-1960. A total of 111 cases of mercury poisoning and 43 deaths were reported among people who had consumed seafood from the bay, which had been contaminated with mercury waste from a chemical plant. Congenital defects were observed in 19 babies whose mothers had consumed seafood contaminated with mercury (Manahan, 2000). This was not the last incident that involved human exposures to heavy metals as there had been other reports regarding such incidents occurring around the globe such as the 'Itai-itai' incident involving contamination of cadmium in Jintsu River in Japan (Sud et al., 2008). Various regulatory bodies have set the maximum prescribed limits for the discharge of toxic heavy metals in the aquatic systems. In Malaysia, the Environmental Quality Act 1974 (Environmental Quality Act 1974 (Act 127)) was established to provide legal provision for project proponents to vary their standards of effluents.

1.2.1 Copper

Copper is widely distributed in nature. It is described as a noble metal because it is rather stable in the elemental state and is reluctant to lose electron and pass into the ionic state. It is also a transition element and shows typical features of variable valency, coloured ions and has tendency to form complex. Copper(II) ions form

stable complexes such as chelates with organic substances and this can cause its effective removal from solution. Two ionic forms, Cu^{2+} (cupric) and Cu^+ (cuprous) are recognised, and the divalent form being much more common (Walker, 1971).

Copper is a low-toxicity, corrosion-resistant metal widely used because of its workability (ductility and malleability), electrical conductivity and ability to conduct heat. In addition to its use as electrical wire, copper is used in tubing, shims, gaskets and other applications (Manahan, 2000). Metallic copper has antibacterial properties and has a biological role in sustaining life. An adult human body consists around 100 mg of copper, mostly attached to protein, and requires an intake of some 3-5 mg per day. Moreover, copper deficiency can result in anaemia (Greenwood and Earnshaw, 1997).

However, accumulation of copper in human body may lead to Wilson's disease, a systemic disease with neurological symptoms and liver damage (Çavuş and Gürdağ, 2008). A higher incidence of stomach cancer in humans has been found in regions where the Zn:Cu ratio in the soil exceeded certain limits. Epidemiological evidence also showed high incidence of cancer among coppersmiths suggesting a primary carcinogenic role of copper (Ho et al., 2002). Intoxication by copper salts resulted in vomiting, hypertension, coma and death. Its toxicity is highly pH dependent and it has been reported to be more toxic to fish at lower pH values. Copper ions are toxic to most forms of life whereby 0.5 mg/L in water is lethal to many algae while most fish succumb to a few parts per million. In Malaysia, according to the Environmental Quality Act 1974, the amount of copper ions present in the industrial effluents and

wastes from development projects that are located within catchments areas, should not exceed 0.20 mg/L (Environmental Quality Act 1974 (Act 127)).

1.2.2 Lead

Lead has been mined in Britain since the time of the Romans. It is a soft metal of high density with an atomic weight of 207 and is commonly encountered as the divalent plumbous ion (Pb^{2+}). Lead is one of the most useful metals due to its wide distribution and its easiness to be extracted and to work with. Lead has many functions, ranging from sheets for roofing to blocks for screening from radioactive emissions. It has also been used as an alloy in electric battery manufacturing and its compounds such as alkyl are used in motor fuels for its anti-knock properties, lead oxides in paints and lead arsenates in insecticides (Lenihan and Fletcher, 1977).

However, lead has the most damaging effects on human health, whereby it can enter the human body through uptake of food (65%), water (20%) and air (15%) (Ho et al., 2002; Nurchi and Villaescusa, 2008). The nervous system, blood cells and kidneys are the parts of the body most affected by lead poisoning, but other organs can also be affected. Symptoms of lead poisoning include abdominal pain, anaemia and lesions of the central and peripheral nervous system which cause behavioural problems. The most damaging long-term effects of lead poisoning occur in children. Children exposed to lead poisoning are affected by convulsions, paralysis and coma at the time of attack, and intellectual impairment later in life (Lenihan and Fletcher, 1977; Rana, 2006). Meanwhile, in adults, the most severe neurological effect of lead

is lead encephalopathy, which is a general term to describe various diseases that affect brain function (Bhattacharyya and Gupta, 2006).

Contaminated water supplies can be a significant source of lead exposure particularly in soft-water areas whereby plumbing systems are made of lead. Lead poisoning arising from domestic water, although seldom severe, has claimed one fatality in 1941, whereby the lead content in the domestic water supply was eight times higher than the present World Health Organization (WHO) limit. In the most recent cases, lead poisoning in rural districts of Scotland was due to the high lead content in tap water (Lenihan and Fletcher, 1977). The presence of lead in industrial effluents and waste from development projects that are located within catchments areas in Malaysia should not exceed 0.10 mg/L, as has been stated in the Environmental Quality Act 1974 (Environmental Quality Act 1974 (Act 127)).

1.3 Treatment Technologies for Heavy Metal Ions Containing Wastewaters

It is a fair hypothesis that a substance which is harmful when present in large amounts over a short period may also be harmful in smaller amounts over a long period. The possible health effects of smaller continual exposures to heavy metals from the environment are now recognized as being very important. In the last decade, various effluent treatment systems for heavy metals containing wastewaters have been proposed including chemical precipitation, ion exchange, reverse osmosis, electrocoagulation, electrodialysis and adsorption.

1.3.1 Chemical precipitation

Chemical precipitation is the most common method for removing toxic heavy metal ions up to parts per million (ppm) levels in water. In Thailand and Turkey, chemical precipitation is used for treating electroplating wastewaters (Tünay and Kabdasli, 1994; Charentanyarak, 1999). Lime or calcium hydroxide (Ca(OH)_2) is the most commonly employed precipitant agent. Lime precipitation can be employed to treat inorganic effluent with concentration of heavy metal ions higher than 1000 mg/L (Kurniawan et al., 2006). Feng et al. (2000) used lime to treat acid mine water obtained from a south African gold mine which contained various heavy metal ions. In the study by Feng et al. (2000), the concentration of calcium, sulphate, barium, phosphate, chloride and fluoride decreased as the precipitation process proceeded. These ions formed low solubility precipitates which was separated using a magnetic separation. However, it was found that iron and manganese could not be precipitated completely owing to its highly soluble precipitates. Powerful oxidants were required to oxidize ferrous iron and divalent manganese as the strongly complexed ions were not readily oxidized with oxygen. Moreover, it was found that it is impossible to achieve a maximum removal for all the heavy metal ions at a specific pH, as different pH was required for the removal of different heavy metal ions. Other interesting findings were reported by Chen et al. (2009), who used lime together with fly ash and obtained percentage of removal up to 97.14 - 98.54 % for copper(II), lead(II), chromium(III) and zinc(II) ions. Chen et al. (2009) used about 900 mg/L of lime to obtain the high percentage of removal. The efficiency of the metal precipitation was high in the broad pH range of 6-12 with the optimum pH value being between pH 8 and 10. Although chemical precipitation is cost effective, its

efficiency is affected by low pH and the presence of other salts (ions). The pH must be strictly controlled as precipitates of amphoteric metals such as zinc and lead tend to re-dissolve as the pH changes beyond the optimum pH range (Chen et al., 2009). This process also requires the addition of other chemicals, which finally leads to the generation of sludge that requires further treatment which is cost intensive (Kurniawan et al., 2006). High dosage of the precipitant agent is required and heavy metal ions may not be reduced to an acceptable level for discharge due to poor settling and dissolution of precipitates (Tadesse et al., 2006). Furthermore, chemical precipitation with lime or bisulphide lacks the specificity and is ineffective to remove metal ions at low concentration (Ahluwalia and Goyal, 2007).

1.3.2 Ion exchange

Ion exchange is another method used successfully in the industry for the removal of heavy metal ions from effluents. Though it is relatively expensive as compared to the other methods, it has the ability to achieve parts per billion (ppb) levels of clean up while handling a relatively large volume of wastewaters (Ahluwalia and Goyal, 2007). Ion exchange is a method to remove cations or anions from solution onto a solid resin, which can be regenerated by treatment with acids, bases or salts (Manahan, 2000). Some of the most commonly used resins are clinoptilolite, Amberlite IR-120, Dowex 2-X4 and zeolite. In Italy and Spain, ion exchange has been used as one of the methods to treat wastewaters laden with heavy metal ions (Pansini et al., 1991; Álvarez-Ayuso et al., 2003). The uptake of nickel(II) ions using clinoptilolite was studied by Papadopoulos et al. (2004). The percentage of removal was up to 74.8 % and was further improved to 98.3 % by using the combination of

ion exchange and precipitation processes. Meanwhile, Lee et al. (2006) compared the efficiency of Amberlite IRC-718 (weak acid cationic chelating exchange resin) and IR-120 (strong acid cationic exchange resin) in removing copper(II), zinc(II), cadmium(II) and chromium(III) ions. The authors found that Amberlite IR-120 had higher adsorption capacity in comparison to Amberlite IRC-718. This showed that a strong cationic ion exchange resin provided more exchangeable sites for heavy metal ions, thus giving better removal efficiency (Lee et al., 2006). Ion exchange can be effectively used to treat inorganic effluent with metal concentration of less than 10 mg/L, or even higher than 100 mg/L. Unlike chemical precipitation, ion exchange does not present any sludge disposal problem therefore lowering the operational costs for the disposal of the residual metal ions sludge (Kurniawan et al., 2006). The disadvantage of this method is that, it cannot handle concentrated metal solution as the matrix gets easily fouled by organics and other solids in the wastewater. Moreover, suitable ion exchanger resins are not available for all heavy metal ions and are highly sensitive to pH of the solution (Kurniawan et al., 2006; Ahluwalia and Goyal, 2007).

1.3.3 Electrocoagulation

Electrocoagulation is an electrochemical approach, which uses an electrical current to remove heavy metal ions from solution. The contaminations present in wastewater are maintained in solution by electrical charges. When these ions and other charged particles are neutralized by ions of opposite electrical charges provided by electrocoagulation system, they become destabilized and precipitate in a stable form. Aluminium, iron and cast iron electrodes are commonly used in the

electrocoagulation system to remove heavy metal ions (Kabdaşli et al., 2009). Merzouk et al. (2009) used aluminium electrodes to treat textile wastewater and for the separation of some heavy metal ions in aqueous solution. Their results showed that high removal efficiency for suspended solid, turbidity, biological oxygen demand and chemical oxygen demand can be achieved at a current density of 11.55 mA/cm² at a retention time of 10 min. Meanwhile, the removal efficiency for iron(II), nickel(II), copper(II), zinc(II), lead(II) and cadmium(II) ions using electrocoagulation were almost 98.5 % although the heavy metal ions concentration was increased from 50 to 400 mg/L. In another study, Kabdaşli et al. (2009) used stainless steel electrodes to treat metal plating wastewater containing nickel(II) and zinc(II) ions. The results obtained by the authors showed that as the current density was increased from 2.25 to 9.0 mA/cm², the total organic content was reduced up to 66 % and a total removal of heavy metal ions was achieved. However, the disadvantage of this system is due to the formation of flocs of metallic hydroxide which requires further purification, making the recovery of valuable heavy metal ions impossible (Kurniawan et al., 2006). This system is also not an economical method for treating wastewaters because of the high electrical energy consumption.

1.3.4 Reverse osmosis

Reverse osmosis is a pressure driven membrane process whereby the heavy metal ions are retained while water pass through the membrane (Kurniawan et al., 2006). The reverse osmosis process requires a driving force to push the fluid through the membrane and the most common force is pressure from a pump. This technique is gaining favourability in Malaysia and Spain (Ujang and Anderson, 1996; Benito and

Ruiz, 2002). Ozaki et al. (2002) studied the performance of an aromatic polyamide (ES 20) ultra-low-pressure reverse osmosis membrane for the removal of copper(II), nickel(II) and chromium(VI) ions in aqueous solution. The authors found that the rejection of heavy metal ions was greater than 99 % at higher feed concentration and pH. The possible reason was that at high pH, heavy metal ions were capable of forming insoluble hydroxide complexes which cannot easily pass through the tighter ES20 membrane. Once the membrane was used to treat electroplating wastewater, the rejection of heavy metal ions was around 98 % which was slightly lower than the rejection of heavy metal ions in the aqueous solution. This was due to the presence of other ions in the wastewater. In the work by Mohsen-Nia et al. (2007), a thin film composite (polyamide) of spiral wound type membrane was successfully used to remove copper(II) and nickel(II) ions in a reverse osmosis system. The authors found that the addition of disodium ethylenediaminetetraacetic acid salt increased the percentage of removal for copper(II) and nickel(II) ions up to 99.5 %. This was because the chelating agent increased the ionic size of copper(II) and nickel(II) ions and thus increasing the efficiency of the removal process using the membrane. The major parameter that affects the extent of heavy metal ions removal using reverse osmosis is pressure. The higher the pressure, the higher is the removal efficiency of heavy metal ions and thus the higher is the consumption of energy. Other than that, the existence of suspended solids or oxidized compounds such as chlorine oxides, will promote membrane fouling which might be irreversible. The membrane would then have to be replaced, thus increasing the operational costs (Kurniawan et al., 2006).

1.3.5 Electrodialysis

In electrodialysis, selective membranes (alternation of cation and anion membranes) are fitted between the electrodes in electrolytic cells and once under continuous electrical current, the associated ion migrates, allowing the recovery of metal ions (Ahluwalia and Goyal, 2007). When a solution containing ionic species passes through the cell compartments, the anions migrate toward the positively charged anode and the cations toward the negatively charged cathode. Tzanetakis et al. (2003) used ion exchange membranes for the electrodialysis of nickel(II) and copper(II) ions from aqueous solution. Two cation exchange membranes, perfluorosulfonic Nafion 117 and sulfonated polyvinylidene fluoride (SPVDF) membrane were compared under similar operating conditions. The SPVDF membrane performed as good as the commercial Nafion 117. According to the authors, the new SPVDF membrane combined low electrical resistance with satisfactory chemical, thermal and mechanical stability and can be used as an alternative low cost membrane to the Nafion 117. Meanwhile, Mohamed (2002) used an electrodialysis method to treat silty clay soil polluted by lead. The author studied the effect of two different chemical reagents on the removal of lead(II) ions from the tested soil. The total removal of lead(II) ions was 80 and 92 % using tap water at pH 4 and sodium acetate at pH 5, respectively. Electrodialysis has the ability to treat wastewater laden with heavy metals ions and for the rejection of undesirable impurities from water. However, as electrodialysis is a membrane process, it requires clean feed and careful operation to prevent any damages to the stack (Kurniawan et al., 2006).

1.3.6 Adsorption

All of the above methods had been found to have disadvantages. Some of the above methods involved high operational costs, especially for the treatment of large volume or highly concentrated effluents and might be insufficient to meet strict regulatory requirements. Adsorption onto solid substrate materials is considered as the most suitable process for the removal of heavy metal ions from solution at low and high concentrations. Activated carbon is one of the most widely employed adsorbents to treat wastewater. It can be used for purification, decolourization and the removal of toxic organics and heavy metal ions (Kim et al., 2001). Commercial activated carbons are prepared from a variety of carbonaceous raw materials. The qualities and characteristics of activated carbons depend on the physical and chemical properties of the starting materials and the activation methods used (Yang and Lua, 2006). The commercial activated carbon can be divided into H- and L-type. The H-type activated carbon are activated at high temperature and adsorb hydrogen ions (H^+), while the L-type activated carbon are activated at low temperature and can adsorb hydroxide ions (OH^-) (Chen and Lin, 2001). The limitation to the usage of activated carbon lies greatly in the high cost of the material and the difficulty of its regeneration after use (Prasad and Saxena, 2004).

Therefore, numerous approaches have been studied for the development of cheaper adsorbents (Varma et al., 2004; Zhao et al., 2007). An adsorbent can be considered low-cost if it requires little processing, is abundant in nature or is a by-product or waste material from another industry (Crini, 2006). Raw agricultural solid wastes and waste materials from forest industries such as sawdust and bark have been widely

used as adsorbents. Sawdust which contains various organic compounds such as lignin, cellulose, and hemicellulose with polyphenolic groups might be useful to bind heavy metal ions through different mechanism (Crini, 2006). Chemically pre-treated sawdust had shown to improve the adsorption capacity (Argun et al., 2007; Meena et al., 2008). Many studies had proven that sawdust is a promising adsorbent for the removal of heavy metal ions (Taty-Costodes et al., 2003; Acar and Eren, 2006; Šćiban et al., 2007; Yasemin and Zeki, 2007; Naiya et al., 2009; Rahman and Islam, 2009). Another waste product from the timber industry to be considered is bark. Bark has been found to be effective in removing heavy metal ions due to its tannin content. The polyhydroxy polyphenol groups of tannins are thought to be active species in the adsorption process (Crini, 2006). Several studies had used bark from different trees for the adsorption of heavy metal ions and showed promising results (Al-Asheh and Duvnjak, 1997; Vázquez et al., 2002; Gundogdu et al., 2009; Naiya et al., 2009). Some of the other raw agricultural solid wastes used for the removal of heavy metal ions from aqueous solution are sugar-beet pulp (Dronnet et al., 1997), tree fern (Ho et al., 2002), *Azadirachta indica* (neem) leaf powder (Sharma and Bhattacharyya, 2004), palm kernel fibre (Ho and Ofomaja, 2005), unmodified and thiolated coconut fibre (Igwe et al., 2008) and rubber (*Hevea brasiliensis*) leaves (Ngah and Hanafiah, 2009).

Other than agricultural and forest industries' solid wastes, industrial solid wastes such as fly ash and red mud are also classified as low-cost materials and can be used for the removal of heavy metal ions. Fly ash, a waste product generated during the burning of coal consists of alumina, silica, ferric oxide and calcium oxide (Ayala et al., 1998; Alinnor, 2007). Its properties are extremely variable and depend strongly

on its origin. Its alkaline property makes it useful in wastewater treatment for the precipitation of metallic ions. Several studies showed the efficiency of fly ash in the removal of heavy metal ions (Ayala et al., 1998; Héquet et al., 2001; Alinnor, 2007; Chen et al., 2009; Wang et al., 2009). Another abundant industrial by-product is red mud. Red mud is an insoluble fine-grained residue of alumina production industry. Some of the major constituents of red mud are Fe_2O_3 , TiO_2 , Al_2O_3 , SiO_2 and Na_2O . Due to its high content of aluminium, iron and calcium content, it has been used as an inexpensive adsorbent for the removal of heavy metal ions in many studies (Gupta, 2001; Vaclavikova et al., 2005).

Biological materials such as chitin, chitosan, peat, yeasts or bacterial biomass are also used to accumulate and concentrate pollutants from aqueous solution. These biosorbents and their derivatives contain a variety of functional groups which can form complex with heavy metal ions (Shahidi et al., 1999). Most of the biosorbents are more selective than traditional ion-exchange resins and commercial activated carbons (Crini, 2006). The adsorption of heavy metal ions using chitin and its deacetylated form, chitosan is one of the emerging methods for removing heavy metal ions even at low concentrations (Vold et al., 2003; Kurita, 2006). These biopolymers have been receiving particular attention because of its structure, physico-chemical characteristics, chemical stability, high reactivity and excellent selectivity towards heavy metal ions, resulting from the presence of hydroxyl, acetamido or amine groups in the polymer chain (Crini, 2005).

1.4 Sources and Properties of Chitin

Polysaccharides are material produced by living beings and are widely distributed in nature. Among the many kinds of polysaccharide found in nature, cellulose and chitin are the most important of all. Cellulose, produced by photosynthesis in plants, composes the largest portion (about 50 %) of the total biomass. Meanwhile, the second most common portion of biomass comes from another polysaccharide, chitin (Mathur and Narang, 1990; Rinaudo, 2008).

The name 'chitin' is derived from the Greek word 'chiton', meaning a coat of mail since it functions as protective coat for invertebrates. Chitin was first described by Braconnot in 1811 who was a professor of Natural History and a member of the Academy of Sciences of Nancy, France (Muzzarelli, 1977). Chitin, $(C_8H_{13}NO_5)_n$, is a linear polymer with high-molecular weight composed of 2-acetamido-2-deoxy- β -D-glucose (N-acetylglucosamine) units. Structurally, chitin (Figure 1.1b) is related to cellulose (Figure 1.1a) with difference only at the C2 carbon, whereby in cellulose it is the hydroxyl group (-OH) while in chitin it is the acetamido group (-NHCOCH₃).

Chitin is the most abundant organic constituent in the skeletal of invertebrates. It was found in arthropods, annelids and mollusks, where it provides skeletal support and body armour (Whistler, 1973). The exoskeletons of crabs and lobsters have been the source of raw material for the production of chitin as the dry arthropod exoskeletons contained about 20 % to 50 % of chitin (Muzzarelli, 1973). Normally, chitin is present in the skin or shell of arthropods as a composite of protein, lipids and calcium carbonates.

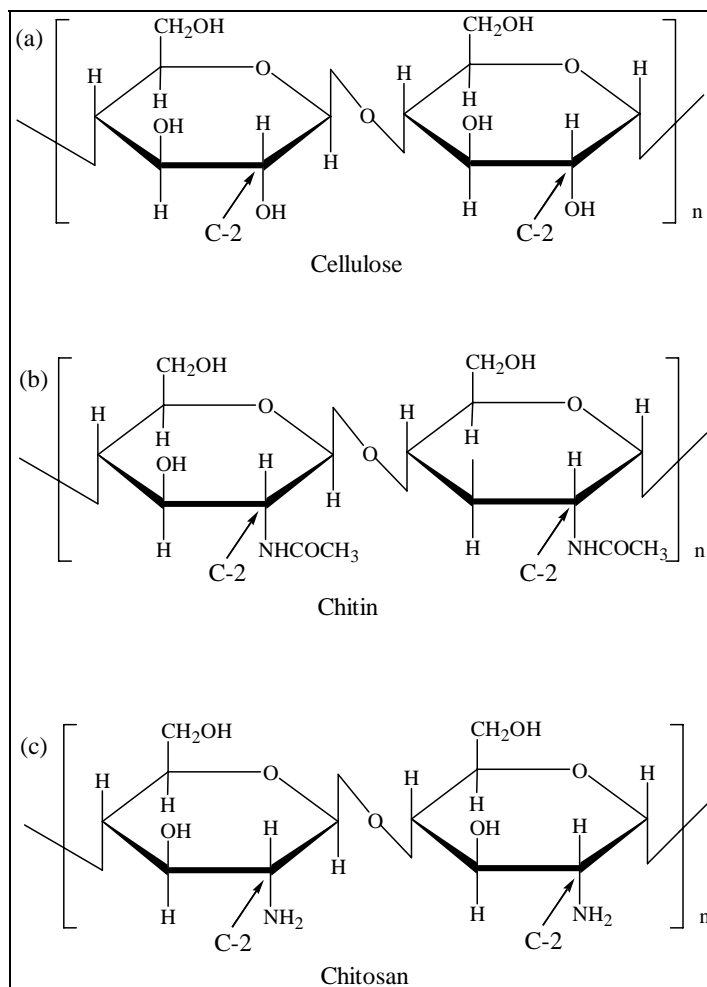


Figure 1.1 Structures of (a) cellulose, (b) chitin and (c) chitosan

The annual worldwide crustacean shells production has been estimated to be 1.2×10^6 tons, and the recovery of chitin and protein from this waste is an additional source of revenue (Crini, 2006). Other potential sources for chitin production include krill, prawn, insects, clams, oysters and jellyfish. Based on Table 1.1, one can remark that the cuticle of the edible crab contains the highest proportions of chitin. Fungi, spores of fungi and mycelia are also potential sources of commercial chitin. Mycelia from some species of *Penicillium* may contain up to 20 % of chitin (Whistler, 1973). Chitin is also found throughout the exoskeletons of most insects, whereby it is

present in amounts ranging up to 60 %. Table 1.1 shows the proportions of chitin found in the wide range of arthropods.

Table 1.1 Proportions of organic components in arthropod cuticles (Muzzarelli, 1973)

Source	Proportions (% of organic fraction; dry weight)	
	Chitin	Protein
<i>Arachnida</i>		
<i>Buthus</i> (scorpion)	31.9	68.1
<i>Mygale</i> (spider)	38.2	61.8
<i>Insecta</i>		
<i>Locusta</i> , clytra and wings	23.7	76.3
<i>Periplaneta</i> (cockroach) av.	35.0	-
<i>Crustacea</i> (Decapodus)		
<i>Cancer</i> (edible crab)	71.4	13.3
<i>Eupagurus</i> (hermit crab)		
Calcified	69.0	31.0
Non-calcified	48.2	51.8

In the production of chitin, shells were first treated with diluted hydrochloric acid at room temperature to remove metal salts especially calcium carbonate which was present in arthropod's shells in high concentration. The decalcified shells were ground and heated at about 100 °C in 1-2 mol/L of sodium hydroxide to decompose proteins and pigments. To ensure the removal of these organic substances, the alkaline treatment was repeated for a few more times and the crude chitin was obtained (Kurita, 2001).

Chitin is a white, hard, inelastic and nitrogenous polysaccharide. The percentage of nitrogen in chitin is theoretically 6.89 % while for artificially substituted cellulose it

is only about 1.25 % or less (Muzzarelli, 1973). The presence of amide groups in chitin is highly advantageous for providing distinctive biological functions and for conducting modification reactions. Chitin is thus expected to have a much higher potential than cellulose in many fields (Kurita, 2001).

The earlier work on the structure of chitin was hampered because of its low solubility. Chitin is highly hydrophobic and is insoluble in water and most organic solvents. However, a partially deacetylated chitin with about 50 % deacetylation prepared under homogeneous conditions is soluble in water (Kurita, 2006). The molecular weight of 143,000 to 210,000 suggested that the molecule has a higher linear array of monomer units. This regularity of structure and the presences of hydrogen bonding and dipole interactions are responsible for the insolubility of natural chitin (Whistler, 1973; Muzzarelli, 1983).

Chitin has low toxicity and it is biodegradable, owing to the presence of chitinases which is widely distributed in nature and is found in bacteria, fungi, plants and in the digestive system of many animals (Rinaudo, 2008). Chitin will degrade before melting, which is typical for polysaccharides with extensive hydrogen bonding (Kumar, 2000). Chitin can be blended with natural or synthetic polymers, it can be cross-linked by cross-linking agents (epichlorohydrin, glutaraldehyde, etc.) or modified by using any other modifications.

Whistler (1973) in his famous treatise predicted that “although chitin is not used commercially now, it is expected that further demands will bring it into industrial use.” True to his prediction, the last one and half decades have seen the commercial

production and utilization of chitin in a host of applications. In addition to that, United States, Japan and India are now manufacturing chitin as a by product from the growing seafood industries. The poor solubility of chitin is the major limiting factor in its utilization. Despite this limitation, various applications of chitin and modified chitin have been reported in medical, pharmaceutical applications and biosensors (Tokura et al., 1990; Eiji and Isao, 1995; Takako and Robert, 1995; Su et al., 1997).

Chitin has also shown its ability to adsorb metal ions and dyes even in acidic solution due to its stability in acidic solution. In the study by Sağ and Aktay (2000), chitin was used to remove chromium(VI) ions in aqueous solution. Chitin particles have also been used effectively for the removal of phenolic dyes whereby the chitin particles adsorbed 2.45 times more dyes than the normally used soil minerals (Felse and Panda, 1999). However, chitin does not exhibit high collection ability as the nitrogen electrons of the amide groups are not available. Due to this, many researchers sought alternative adsorbents which have higher affinity for metal cations. Chitosan, the deacetylated product of chitin, became the best candidate for this purpose because of its high amine groups content (Muzzarelli, 1973).

1.5 Chitosan

Chitosan is the name used for low acetyl substituted forms of chitin and is composed of primarily of glucosamine, 2-amino-2-deoxy- β -D-glucose. Chitosan was first discovered by Rouget in 1859. He found that chitin which has been boiled in a very concentrated potassium hydroxide solution became soluble in organic acids. Modified chitin was studied again by Hoppe-Seyler in 1894 who named it chitosan.

Chitosan is a non-toxic and a biodegradable polymer. The composition and structure of chitosan is very similar to cellulose, except for the difference at the C2, whereby in chitosan, the hydroxyl group is replaced by a primary amine group (Figure 1.1c) (Sandford and Hutchings, 1987). Most of the polysaccharides, e.g., cellulose, dextran, pectin, alginic acid and heparin are neutral or acidic, but chitosan and chitin are the only abundant basic polysaccharides.

Removal of N-acetyl groups from chitin to produce chitosan requires concentrated alkali. A typical deacetylation bath may consist of two parts of potassium hydroxide to one of 95 % ethanol and one of ethylene glycol. The mixture is usually heated to 120 °C. During the deacetylation reaction, some alkaline cleavage of the polysaccharide occurs accompanied by a decrease in the viscosity. Consequently, the reaction is terminated as soon as the acetyl content has been diminished to low levels (Whistler, 1973).

Pure chitosan is rarely found in nature, but it is present in *Zygomycetes* cell walls. It is formed by the action of a chitin deacetylase on the precursor chitin (Kurita, 2001). At the present moment, the most frequently used industrial source of chitosan is chitin.

1.5.1 Properties of chitosan

Chitosan is an amorphous solid, almost insoluble in water but soluble in aqueous organic (formic and acetic acid) and inorganic acids, to give a viscous solution. The solubilization occurs due to the protonation of the amine ($-NH_2$) functional groups

on the C2 position of the D-glucosamine unit. Chitosan is one of the few naturally occurring cationic polyelectrolytes (Rinaudo, 2008). Key properties of chitosan can be divided into three main properties, which are its cationic, biological and chemical properties. Table 1.2 provides a general view of these three properties of chitosan.

Table 1.2 Key properties of chitosan (Sandford and Hutchings, 1987; Crini and Badot, 2008)

Properties	Description
Cationic	<ul style="list-style-type: none"> • The positive charge of chitosan interacts strongly with negative surfaces (proteins and anionic polysaccharides) to give an electrical neutrality • Excellent flocculants due to its vast number of protonated amine groups ($-\text{NH}_3^+$) which interact with negatively charged colloids, such as hair and skin (which are composed of negatively charged mucopolysaccharides and proteins) • Entrapment and adsorption properties; filtration and separation
Biological	<ul style="list-style-type: none"> • Biocompatible <ul style="list-style-type: none"> - Non-toxic - Biodegradable - Natural polymer • Bioactivity <ul style="list-style-type: none"> - Wound healing accelerator - Reduce blood cholesterol - Stimulate the immune system - When coated on seeds, it resulted in increased crop yields. This is due to chitosan which induces protective response by the germinating plant
Chemical	<ul style="list-style-type: none"> • Linear polyamine • Reactive amine ($-\text{NH}_2$) and hydroxyl ($-\text{OH}$) groups • Weak base; the amine groups acts as a powerful nucleophile (pK_a 6.3) • Numerous reactive groups for chemical activation and cross-linking • Chelating and complexing properties • Capable of forming hydrogen bonds intermolecularly

1.5.2 Applications of chitosan

The three key properties mentioned in Section 1.5.1, are now being exploited in several major research areas, including textiles, medical, cosmetics, biotechnology, agriculture and environmental applications (Gerente et al., 2007). Chitosan has important applications in cosmetic as chitosan is the only natural cationic gum that becomes viscous on being neutralized with acid. Due to this, chitosan and several of its derivatives are used in creams, lotions, permanent waving lotions and as nail lacquers (Kumar, 2000). Apart from that, chitosan has important applications in photography due to its resistance to abrasion, its optical characteristics and film forming ability (Muzzarelli, 1983; Kumar, 2000). Application of chitosan film in the extension of the storage life and better control of decay of peaches, Japanese pears and kiwi fruits has been well documented. Chitosan film is tough, long-lasting, flexible and very difficult to tear. Cucumbers, bell peppers, strawberries and tomatoes could also be stored for longer periods after coating with chitosan (Shahidi et al., 1999). Chitosan, with its partial positive charge, can effectively function as a polycationic coagulant in wastewater treatment particularly in removing proteins from wastewaters (Shahidi et al., 1999). Chitosan has also been used as flocculants to treat kaolin suspension, sugarcane molasses and wastewater containing starch from rice processing plants (Muzzarelli, 1983).

Recently, many research involving chitosan have been generated due to the ability of chitosan to remove heavy metal ions from wastewaters through adsorption process. Chitosan has demonstrated the potential to adsorb significant amounts of heavy metal ions and this has generated a large amount of interest in assessing its feasibility to

remove heavy metal ions over a wide range of effluent systems and types (Gerente et al., 2007). In Japan, the capacity of chitosan to form complexes with heavy metal ions has been exploited for water purification, while, the use of commercially available chitosan for potable water purification has been approved by the United States Environmental Protection Agency up to a maximum level of 10mg/L (Shahidi et al., 1999).

The amine groups of chitosan serve as the major adsorption sites for the adsorption of metal ions although hydroxyl groups may also play some part. At near neutral condition, the lone pair of electrons on the nitrogen atoms of amine groups will form dative bond with metal cations. Meanwhile under acidic conditions, the protonated amine groups will bind with anions through electrostatic forces. One of the most interesting advantages of chitosan is its versatility. Chitosan can be physically and chemically modified. These modifications can improve the metal adsorption properties while preventing the dissolution of this polymer when heavy metal ions adsorption was performed in acidic solutions. Currently, many of the research works conducted on chitosan are focused on the modified chitosan.

1.6 Modifications of Chitosan

1.6.1 Physical modification of chitosan

Physical modifications can increase the adsorption properties of chitosan flakes (Chang and Juang, 2004). Derived from a standard alginate beads formation procedure, the physical modification involves dissolution of chitosan flakes in acetic